B2M17NKA - Project II

17TH January, 2024 Martin Šimák

Task *Design of a multi-band mobile phone antenna*

1. Design the following two antennas and create their models in an electromagnetic simulator.
   A. *Planar F-Inverted Antenna (PIFA)* for two (optionally three) bands: E-GSM (880 to 935 MHz), DCS (1710 to 1880 MHz), optionally UMTS (1920 to 2170 MHz). The antenna should achieve the resonation of $|\Gamma(f)| < -12\,\mathrm{dB}$ on the resonating bands centre frequencies.
   B. *Electrically small, folded monopole with a capacitive load* of two different lengths: $\lambda_0/10$ and $\lambda_0/20$. Design the antenna to work on the resonant frequency assigned in Project I. The antenna should achieve the resonation of $|\Gamma(f)| < -15\,\mathrm{dB}$ on the resonant frequency $f_{\mathrm{res}} = 1.8\,\mathrm{GHz}$.
2. Fabricate antenna A with the help of the department. Assume a realistic size of the ground plate corresponding to the dimensions of a mobile phone. The ground plate will be the dielectric substrate Isola IS400 of dimensions $60 \times 120 \times 1\,\mathrm{mm}$, with one-sided copper cladding. The shorting pin will be present in the form of an iron, 10 mm high distance pillar – a hexagonal prism with 5 mm distance between opposing edges. The antenna will be fed be an SMA connector (dimensions in the attached drawing) stripped of the Teflon (PTFE) dielectric beyond the flange. The conductive pattern will be cut out of a thin (thickness $35\,\mu\mathrm{m}$) copper foil using a plotter. This adhesive foil will be contacted onto a thin (thickness 0.5 mm) PET-G dielectric plate which will be placed on top of the iron distance pillar serving as a short.

   During the design, special attention should be paid to the practical feasibility of fabrication, namely the dimensions of the SMA connector and the shorting pin, making a hole for the SMA-feed centre pin etc. Determine the required minimum distance of the centre of the shorting pin from the centre pin of the connector.

Antenna component	Substrate	ϵ_r [−]	$\tan(\delta)$ [−]
Ground plate	Isola IS400	3.9	0.02
Pattern-carrying plate	PET-G	2.4	0.02
Plastic distance pillars	Polyamide	4	0.05

Table 1: Construction parameters of the PIFA components

3. Measure the reflection from the fabricated antenna in the operating frequency bands.
4. Plot the important antenna parameters of all designed antennas:
   4.1 reflection coefficient (simulated, include measured for antenna A),
   4.2 input impedance (simulated, include measured for antenna A),
   4.3 3D radiation patterns and cuts in the E- and H-plane (simulated, both bands for antenna A).
5. Determine the fundamental limits in the design bands.

5.1 Plot the Chu's limit $Q_{\mathrm{min}}(ka)$ using the relations from McLean, Thal and Gustafsson[1] for $ka \in [0.1, 1]$.

5.2 Calculate the quality factors Q_{3dB} and Q_Z (Yaghjian and Best, IEEE TAP, 2005) for all (simulated and measured) antennas from the input impedance $Z_{\mathrm{in}}(\omega)$ and add them to the plot mentioned above.

5.3 Summarize the parameters ka, Q_{3dB}, $Q_{\mathrm{3dB}}/Q_{\mathrm{min}}$, Q_Z, Q_Z/Q_{min}, $BW_{3\,\mathrm{dB}}$ and BW_{Q_Z} of the designed radiators in a table and discuss the effectiveness of their miniaturization. Assume 100 % antenna efficiency and $Q_{\mathrm{min}} = Q_{\mathrm{Gustafsson}}$. Discuss the applicability and suitability of the individual limits.

[1] Determine γ_1^{norm} for the used geometry of the modelled radiators.

1 Antenna models

All the antennas were designed in CST Studio Suite in accordance with the respective assignments. The final models are shown in Figure 1.

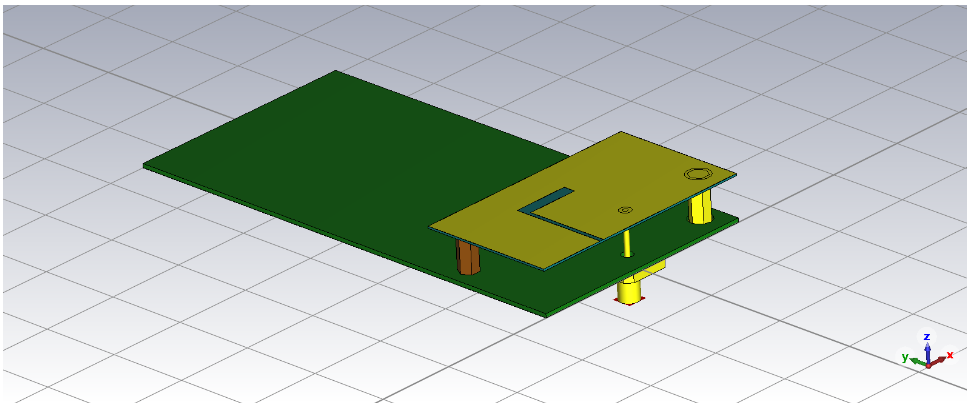

(a) PIFA

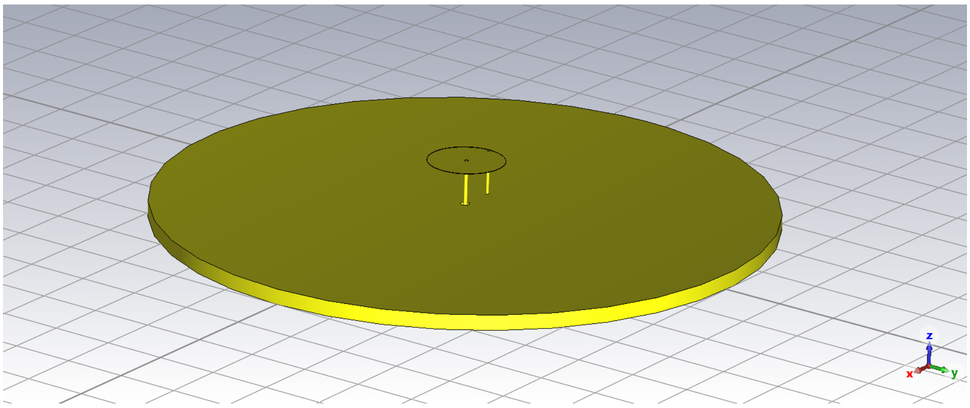

(b) $\lambda/10$ monopole

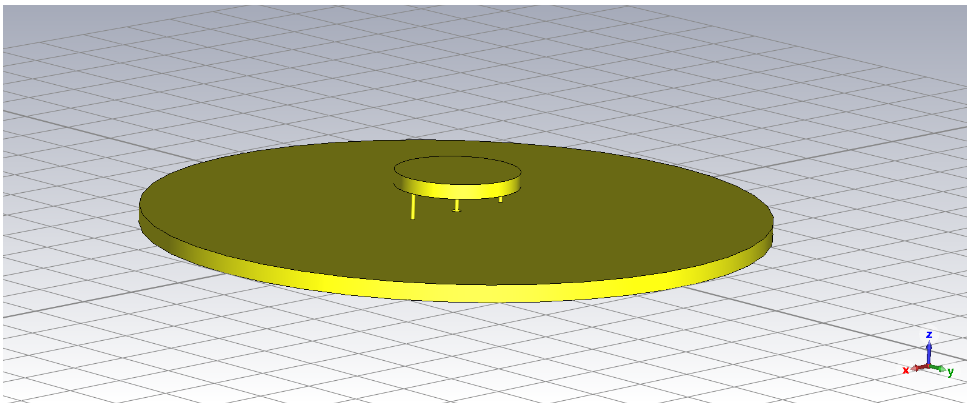

(c) $\lambda/20$ monopole

Figure 1: Antenna models

2 PIFA fabrication

Antenna A (PIFA) has been successfully fabricated in one of the laboratory seminars during the semester. The final product is shown in Figure 2. The distance of the centre of the shorting pin from the centre pin of the connector is 22.8 mm.

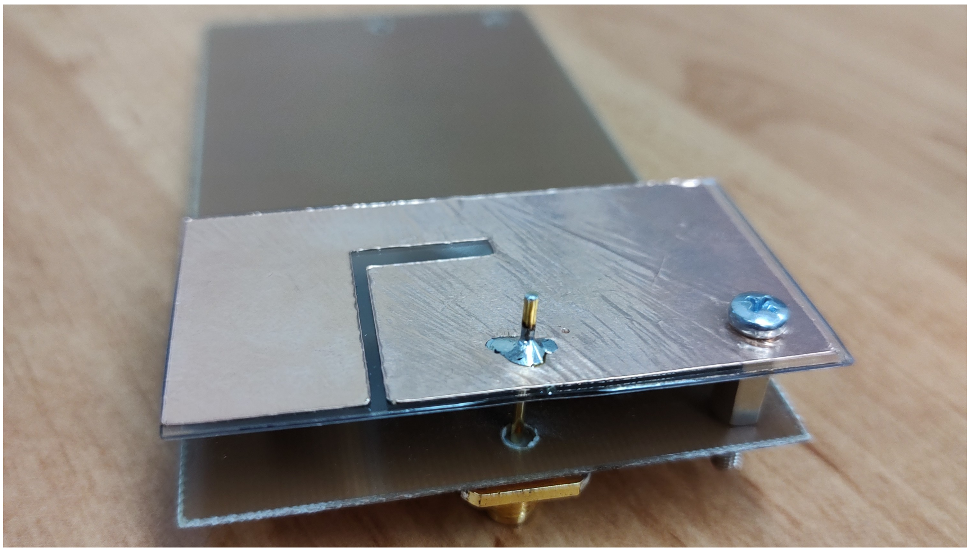

Figure 2: PIFA: fabrication

3 Fabricated PIFA reflection measurement

The input impedance of the fabricated antenna A was determined from the S-parameters (reflection coefficient) measured using a VNA. The measured data is shows in Figure 3.

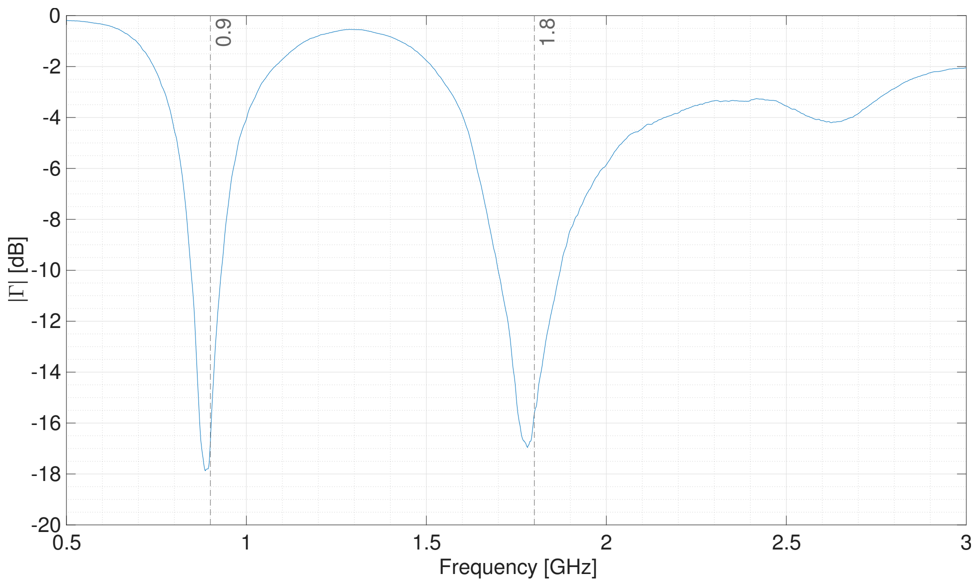

Figure 3: PIFA: reflection measurement

4 Important antenna parameters

PIFA The antenna was both designed and fabricated to the fulfilment of the assignment. This can be seen in Figure 4 where the magnitude of the reflection coefficient clearly reaches the expected values around both resonant frequencies. Furthermore, the complex reflection coefficient is shown using a Smith chart in Figure 5 and the input impedance is plotted by parts in Figure 6. The radiation properties are conveyed both in 3D and 2D. Figure 7 and Figure 10 show the 3D farfield pattern in the lower band and the upper band respectively. The radiation patterns can also be inspected in cuts through the E-plane in Figures 8 and 11 for each band separately and through the H-plane in Figures 9 and 12.

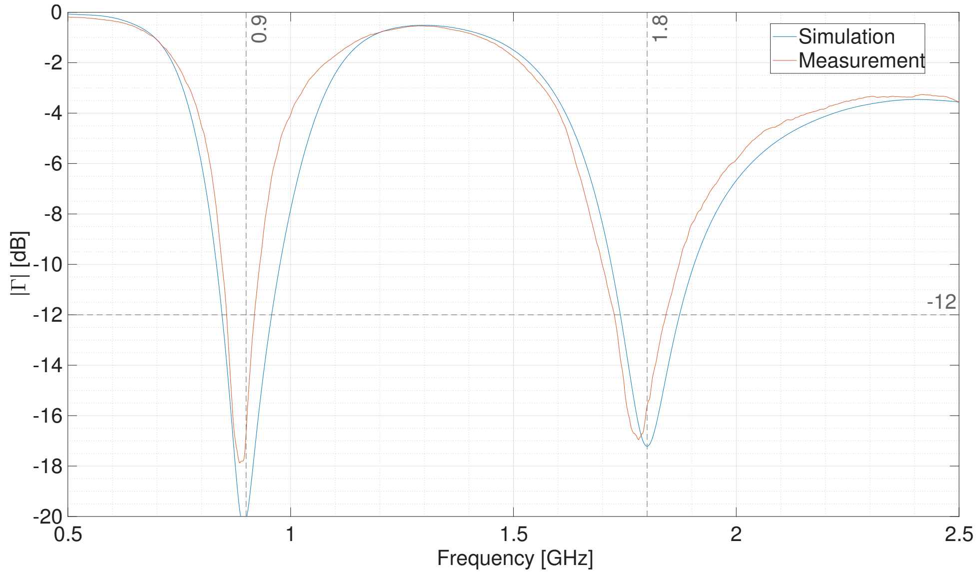

Figure 4: PIFA: Reflection coefficient in the linear scale

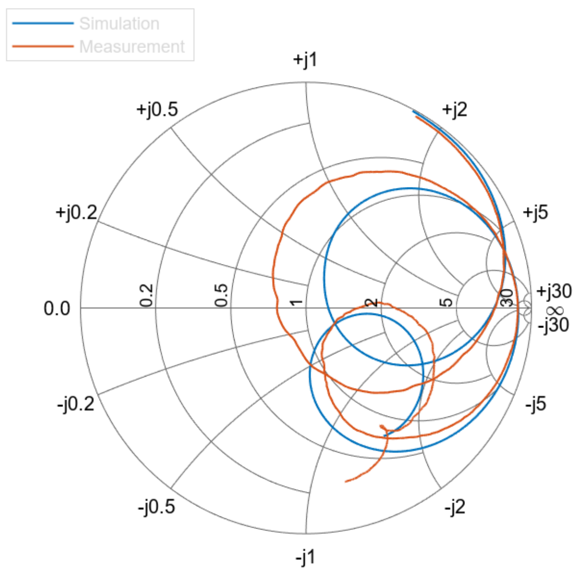

Figure 5: PIFA: Reflection coefficient in the Smith chart

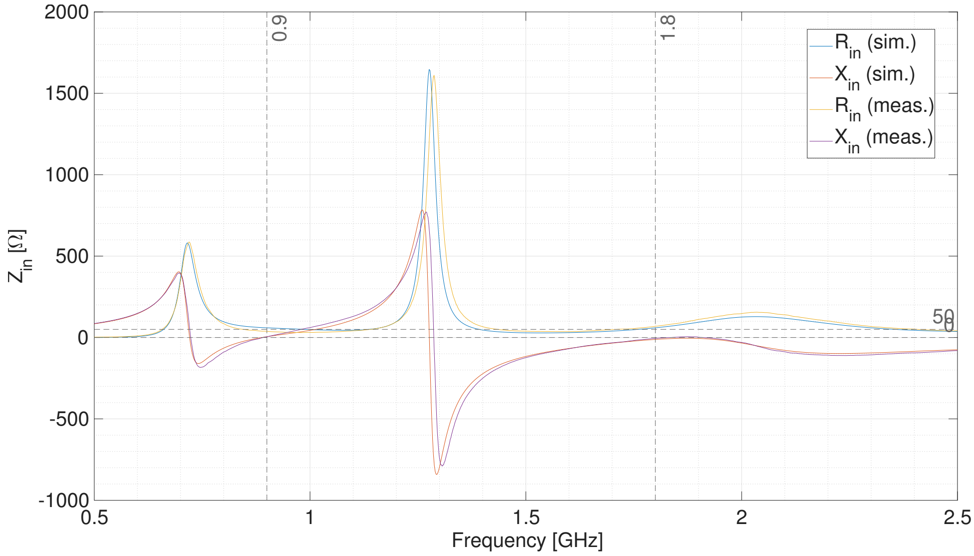

Figure 6: PIFA: Input impedance

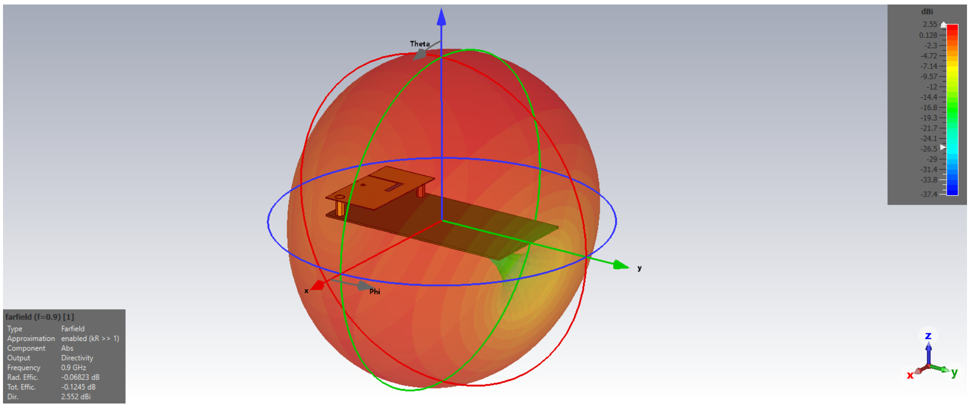

Figure 7: PIFA: farfield in the lower band (0.9 GHz)

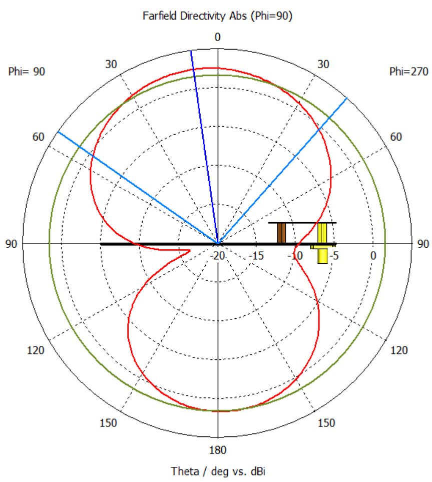

(a) Simulation

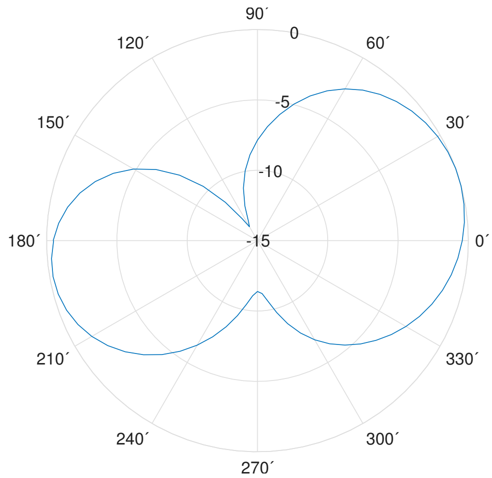

(b) Measurement

Figure 8: PIFA: E-cut of the radiation pattern in the lower band (0.9 GHz)

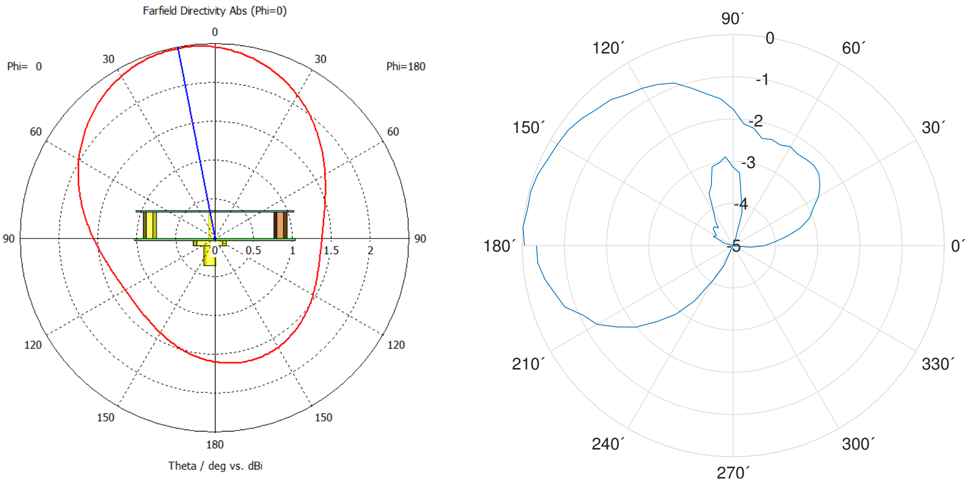

(a) Simulation (b) Measurement

Figure 9: PIFA: H-cut of the radiation pattern in the lower band (0.9 GHz)

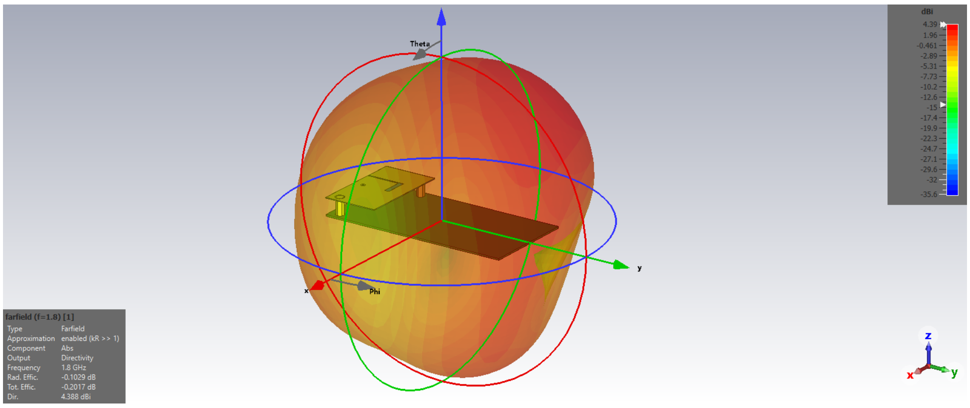

Figure 10: PIFA: farfield in the upper band (1.8 GHz)

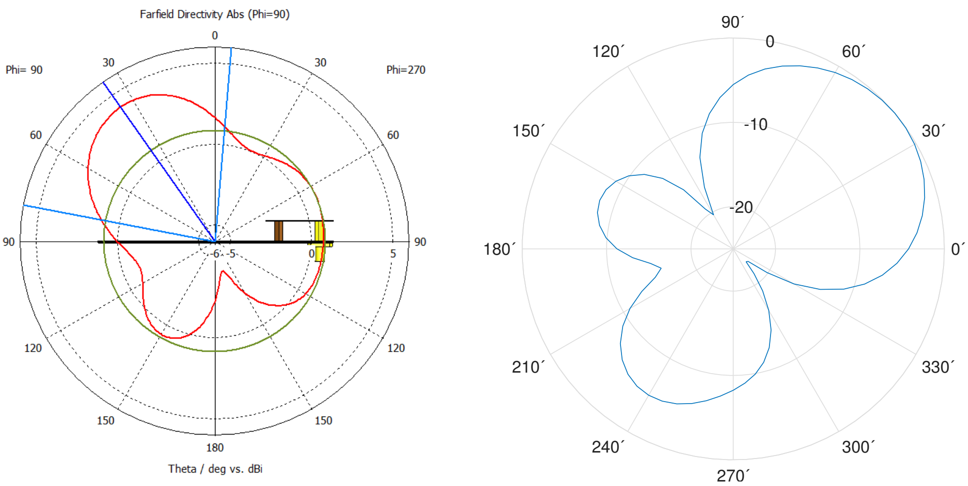

(a) Simulation (b) Measurement

Figure 11: PIFA: E-cut of the radiation pattern in the upper band (1.8 GHz)

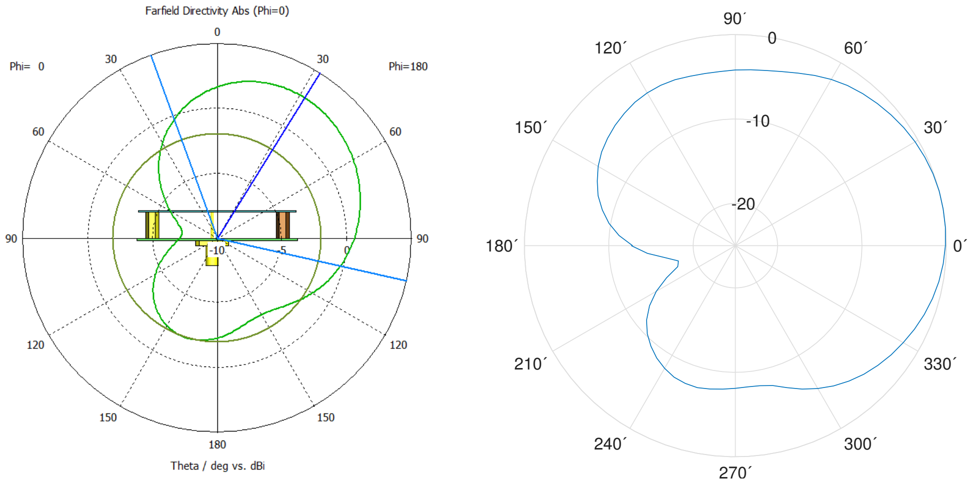

(a) Simulation (b) Measurement

Figure 12: PIFA: H-cut of the radiation pattern in the upper band (1.8 GHz)

Lambda-tenth monopole The antenna was designed to the fulfilment of the assignment. This can be seen in Figure 13 where the magnitude of the reflection coefficient clearly reaches the expected values around both resonant frequencies. Furthermore, the complex reflection coefficient is shown using a Smith chart in Figure 14 and the input impedance is plotted by parts in Figure 15. The radiation properties are conveyed both in 3D and 2D. Figure 16 shows the 3D farfield pattern. The radiation patterns can also be inspected in cuts through the E- and H-plane in Figure 17.

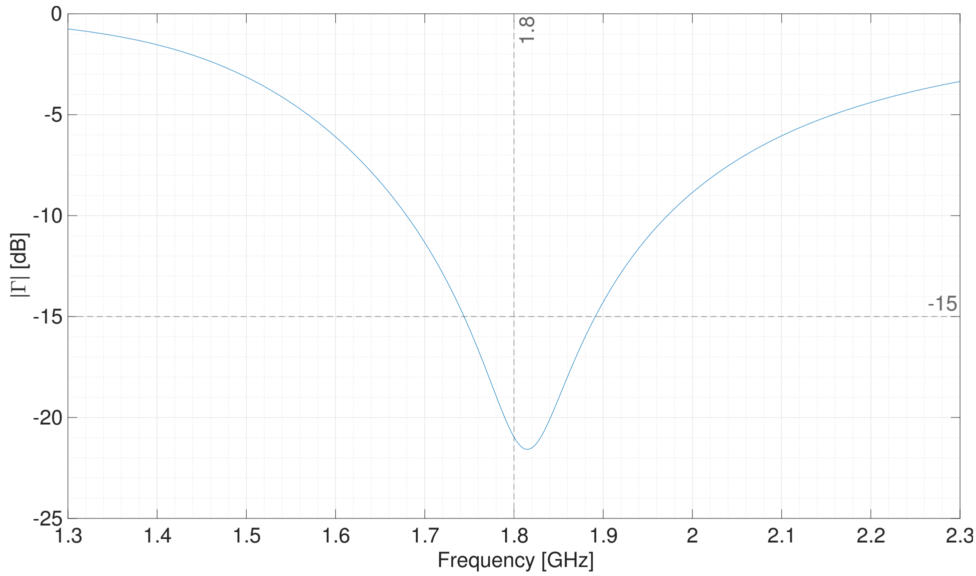

Figure 13: Lambda-tenth monopole: Reflection coefficient in the linear scale

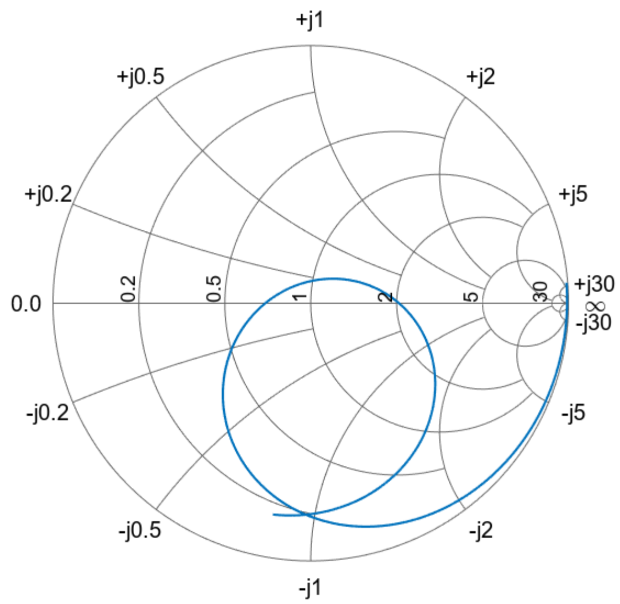

Figure 14: Lambda-tenth monopole: Reflection coefficient in the Smith chart

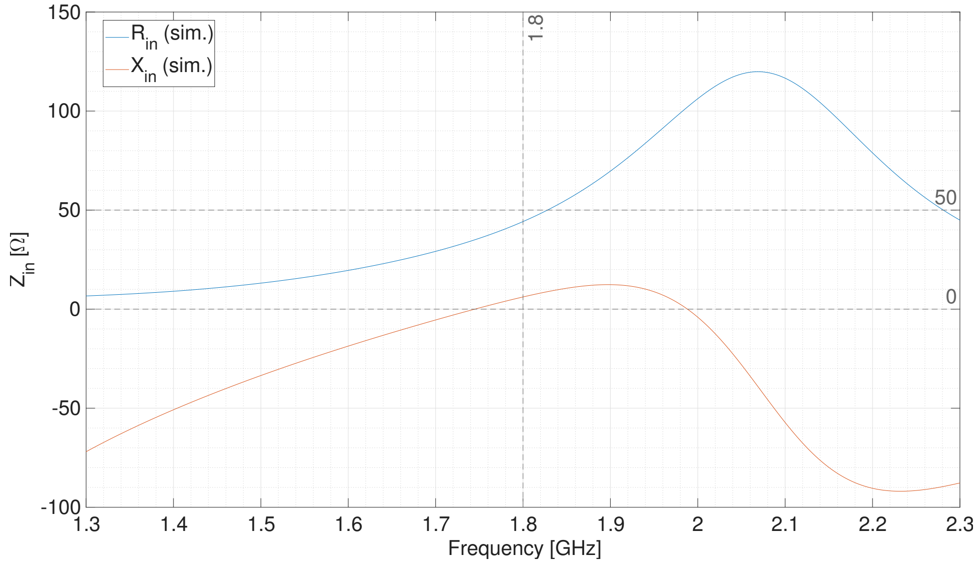

Figure 15: Lambda-tenth monopole: Input impedance

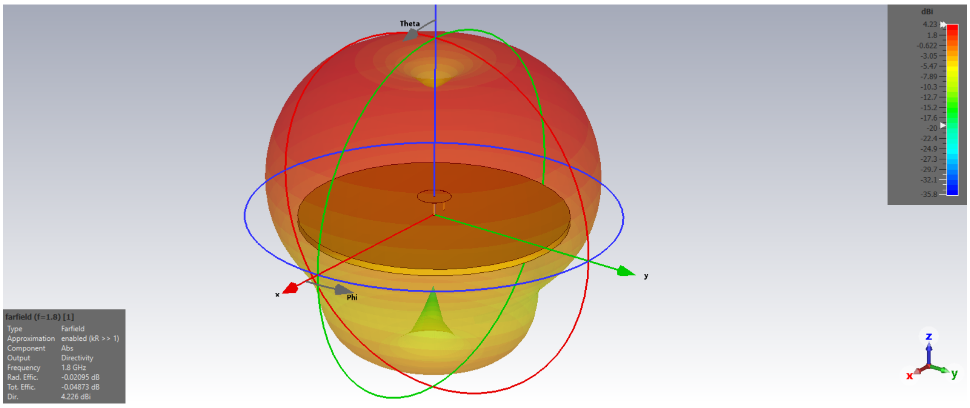

Figure 16: Lambda-tenth monopole: farfield

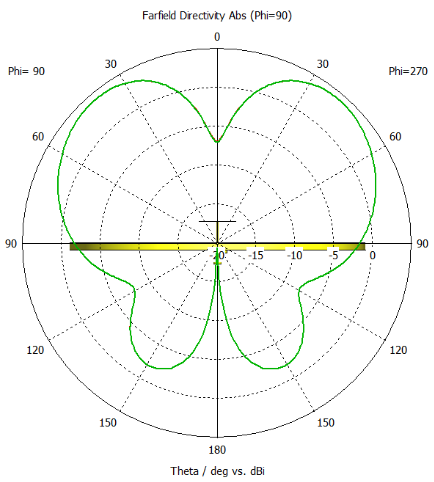

(a) E-plane

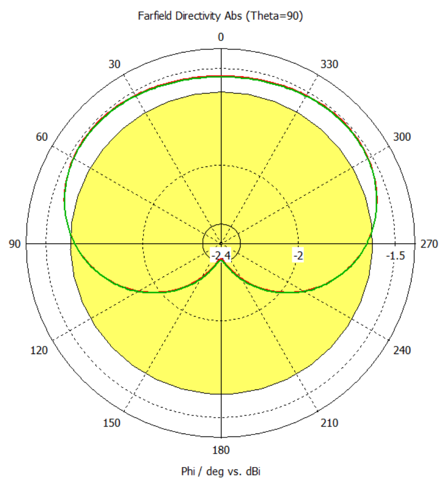

(b) H-plane

Figure 17: Lambda-tenth monopole: radiation pattern cuts

Lambda-twentieth monopole The antenna was designed to the fulfilment of the assignment. This can be seen in Figure 18 where the magnitude of the reflection coefficient clearly reaches the expected values around both resonant frequencies. Furthermore, the complex reflection coefficient is shown using a Smith chart in Figure 19 and the input impedance is plotted by parts in Figure 20. The radiation properties are conveyed both in 3D and 2D. Figure 21 shows the 3D farfield pattern. The radiation patterns can also be inspected in cuts through the E- and H-plane in Figure 22.

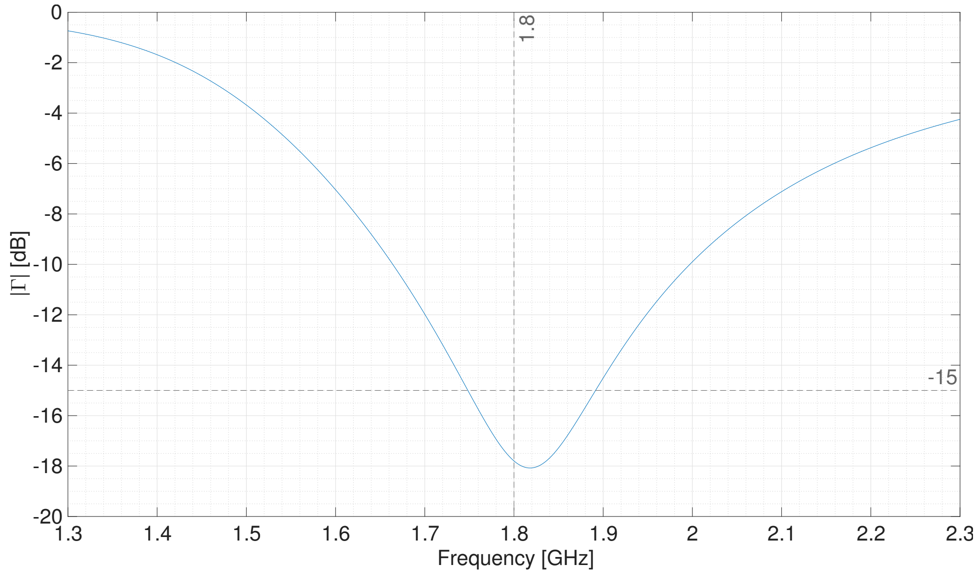

Figure 18: Lambda-twentieth monopole: Reflection coefficient in the linear scale

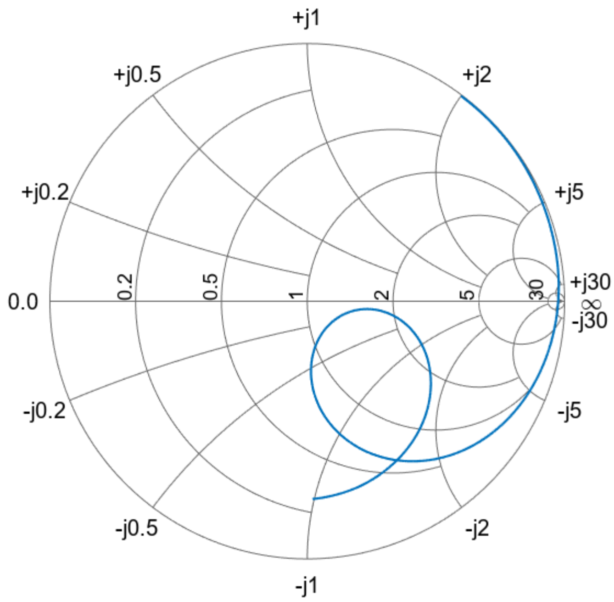

Figure 19: Lambda-twentieth monopole: Reflection coefficient in the Smith chart

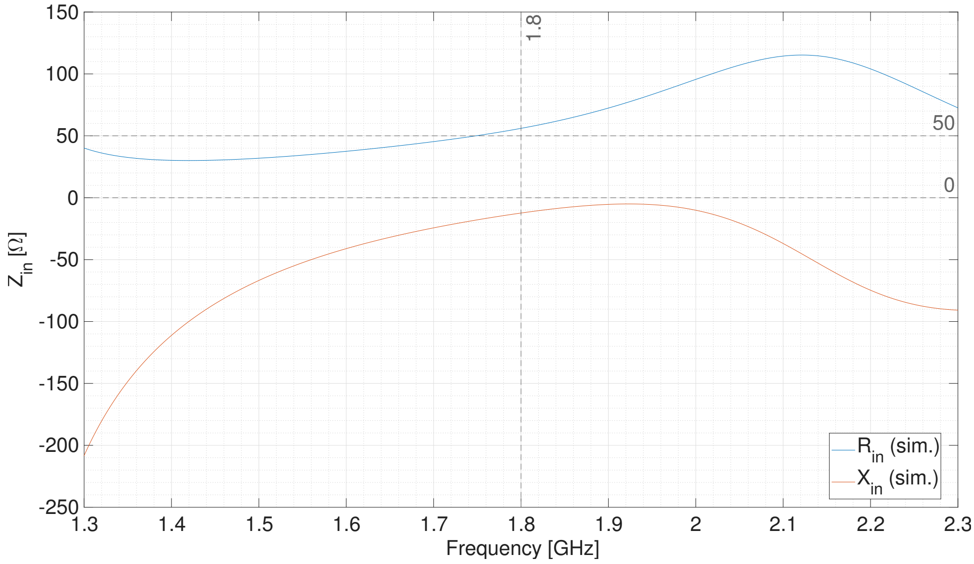

Figure 20: Lambda-twentieth monopole: Input impedance

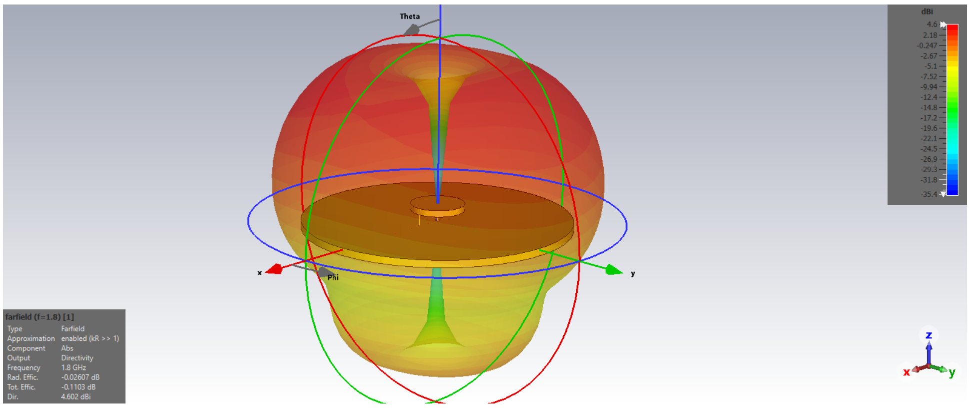

Figure 21: Lambda-twentieth monopole: farfield

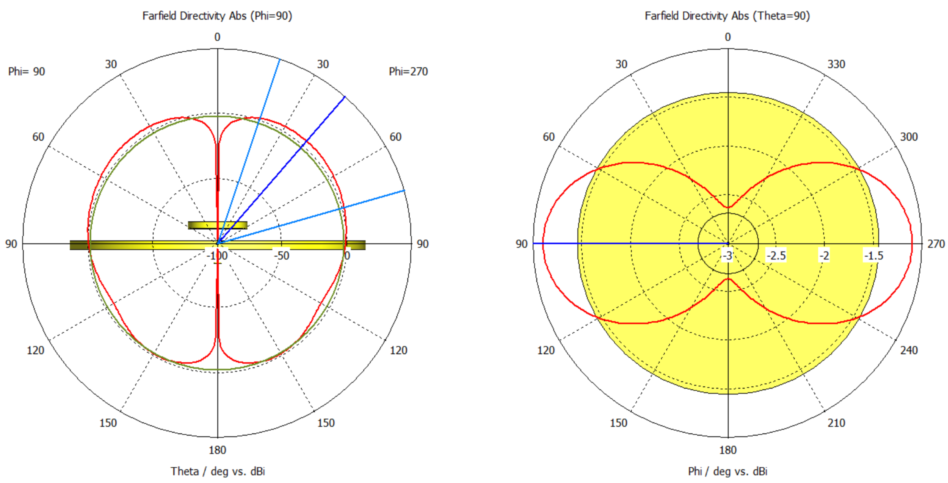

(a) E-plane

(b) H-plane

Figure 22: Lambda-twentieth monopole: radiation pattern cuts

5 Fundamental limits in the design bands

The Chu's fundamental limit of the quality factor with respect to the product ka has been calculated according to the theoretical formulas

$$Q_{\text{McLean}} = \frac{1}{(ka)^3} + \frac{1}{ka}, \qquad Q_{\text{Thal}} \approx \frac{1.5}{(ka)^3} + \frac{0.6}{ka}, \qquad Q_{\text{Gustafsson}} = \frac{1.5}{(ka)^3 \gamma_1^{\text{norm}}}, \tag{1}$$

where γ_1^{norm} can be determined using available analytical formulas. Furthermore, quality factors of the designed antennas have been determined as $Q_{3\text{dB}}$ from the 3 dB drop in reflection and Q_Z from the input impedance using the formula

$$Q_Z(\omega) = \frac{\omega}{2R_{\text{in}}(\omega)} \left| Z'_{\text{in}}(\omega) \right|. \tag{2}$$

The resulting quality factors and their theoretical limits are shown in Figure 23 for both ways of determination.

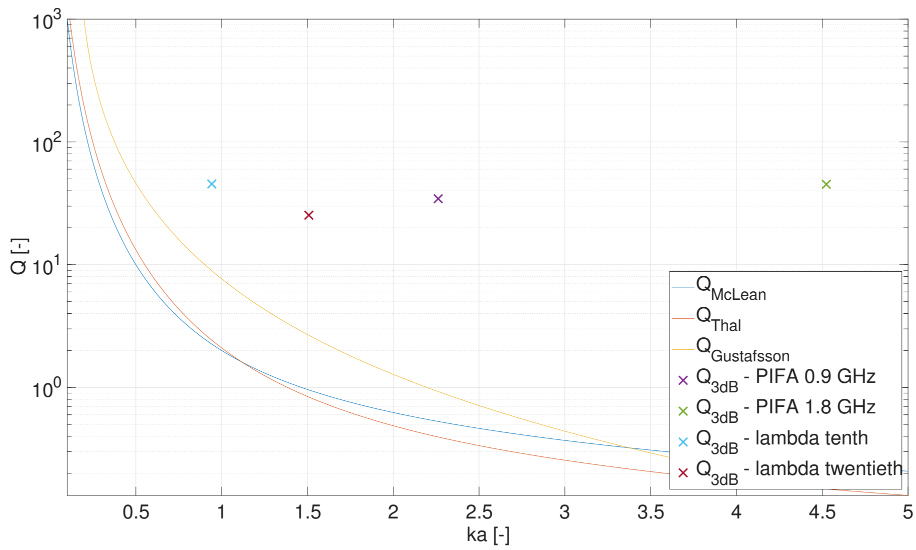

(a) Quality factors calculated from the 3 dB drop in reflection

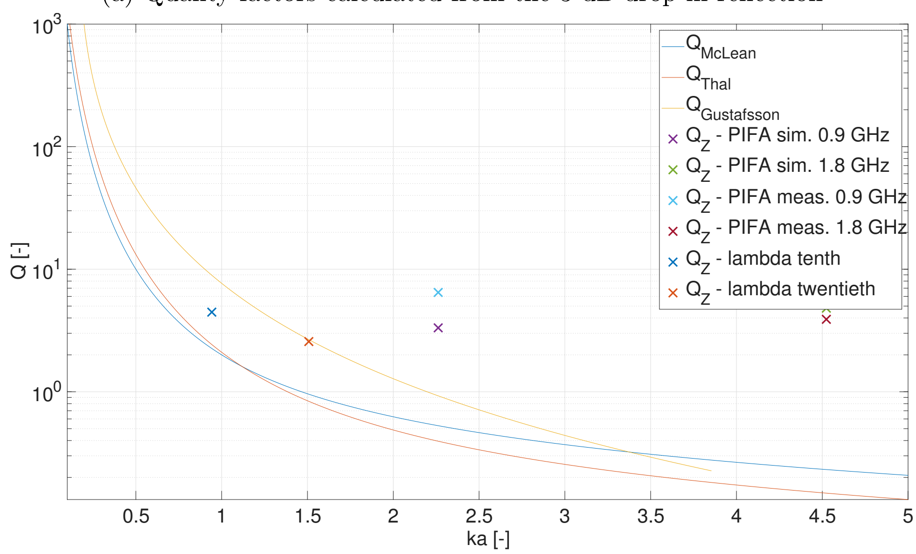

(b) Quality factors calculated from input impedance

Figure 23: Quality factors and their fundamental limits

Discussion The final resonance parameters including the quality factors (and their normalization to the Gustafsson's limit) and the resultant bandwidths are shown in Table 2 for the calculation from the 3 dB drop in reflection and in Table 3 for the calculation from input impedance.

Source	$ka\,[-]$	$Q_{3\text{dB}}\,[-]$	$Q_{3\text{dB}}/Q_{\min}\,[-]$	$BW_{3\text{dB}}\,[\%]$
PIFA (sim.) 0.9 GHz	2.26	34.47	37.43	5.82
PIFA (sim.) 1.8 GHz	4.52	45.16	199.45	4.44
$\lambda/10$ monopole	0.94	45.46	5.16	4.41
$\lambda/20$ monopole	1.51	25.31	9.5	7.92

Table 2: Resonance parameters calculated from 3 dB drop in reflection

Source	$ka\,[-]$	$Q_Z\,[-]$	$Q_Z/Q_{\min}\,[-]$	$BW_Z\,[\%]$
PIFA (sim.) 0.9 GHz	2.26	3.32	3.61	20
PIFA (sim.) 1.8 GHz	4.52	4.81	21.24	14
PIFA (meas.) 0.9 GHz	2.26	8.78	9.53	8
PIFA (meas.) 1.8 GHz	4.52	11.31	49.97	6
$\lambda/10$ monopole	0.94	4.46	0.51	15
$\lambda/20$ monopole	1.51	2.57	0.96	26

Table 3: Resonance parameters calculated from input impedance

As we can see from the fundamental limits shown in Figure 23, the quality factor is inversely proportional to the product ka. This implies that smaller antennas attain higher quality factor. This, however, brings issues in terms of low radiation efficiency and narrow bandwidth.